

## **NUMERICAL SIMULATION OF CATENARY ACTION IN COLD-FORMED STEEL SHEETING IN FIRE**

Wei Lu, Pentti Mäkeläinen  
Jyri Outinen

Journal of Structural Mechanics  
Vol. 40, No. 3, 2007, pp. 28-37

### **ABSTRACT**

A 3-D finite element model incorporating both geometric and material non-linearity is created for investigating the behaviour of cold-formed steel sheeting in fire. After validation of the model, it has been shown that due to the thinness of the material and degradation of material properties at elevated temperature, the profile buckles early under thermal expansion. The steel sheeting can survive in fire (fire rating R 30) by developing tensile force in large deformation with totally opening of profile. The catenary force in the structure has significant role to sustain the transversally applied load. No run-away deformation happened before 30 minutes.

### **INTRODUCTION**

The resistance of steel beam in fire is calculated according to flexural bending behaviour with small deflection and without considering the effects of end axial restraints. This practice of evaluating fire resistance of beam is based on traditional standard fire tests on simply supported individual beams. In real structure, the surrounding members restrain the beams both axially and rotationally. With the presence of axial constraints, the beam will behave in catenary action at large deflection stage. The catenary action is a load carrying mechanism where the bending moment capacity of the beam is negligible but the beam will still be able to resist the applied transversal load with the tension force developed in the beam via further deflection even with reduced material strength, Wang (2002). If large deflection is acceptable in practice, the fire protection might be unnecessary. If the maximum value of this axial tension force is well recognized, it will reduce the damage to the surrounding members.

Currently, three methods are available in researching the catenary action of beam in fire, i.e. testing, numerical simulation with Finite Element (FE) analysis and development of analytical formulation. Testing on axially restrained beam, Liu et al (2001 and 2002), provides the physical understanding of the catenary action and can be used as a validation tool for numerical and analytical analysis. For economical reason, the finite element analysis is used as an alternative of the fire testing. After the validation, the

finite element analysis has been used as the tool to investigate the effects of such parameters as temperature distribution, spans of sheeting, material properties and applied load level on the catenary action, Ying (2004) and Wong (2005). The numerical simulation can provide a clear understanding of the behaviour, however, it is not practical to use as a design tool. Therefore, the analytical analysis is performed to determine the largest deflection and largest catenary force to avoid the complication, Wang and Yin (2006), Allam (2002), Rotter and Usmani (2000) and Usmani et al (2001). The researches on catenary action are mostly for the hot-rolled beam in the framed structure because of the available testing data and popularity of framed structures.

The load bearing deck with insulation on the top is a very popular roof system in industrial buildings. If the load-bearing deck can survive in the large deflection stage in fire, the expensive fire protection can be removed or reduced due to large covering area of the roof. Currently, few researches are available on this topic, Sokol et al (2006).

In this paper, the numerical simulations for two-span sheeting with overlap in the mid-support and for one-span sheeting are carried out. With this simulation, it provides an initial data for guiding further testing of the same type of roof system and initial understanding of the behaviour of cold-formed roof sheeting in fire. If the numerical model can be validated with future testing, it can be used as a tool to make the further parametric investigation.

## INSULATED METAL DECK ROOFING

The insulated metal deck roofing, also called warm roof, is mostly used for industrial buildings with low pitched roof areas, ECCS (1983), and is composed of primary three components: the steel deck itself, the insulation and fasteners or adhesive and the weather resistant roof as shown in Figure 1. In many cases a thin sheet vapour barrier is located between the deck and the insulation to prevent warm humid air from within the building from condensing on the insulation, Zalosh (2003).

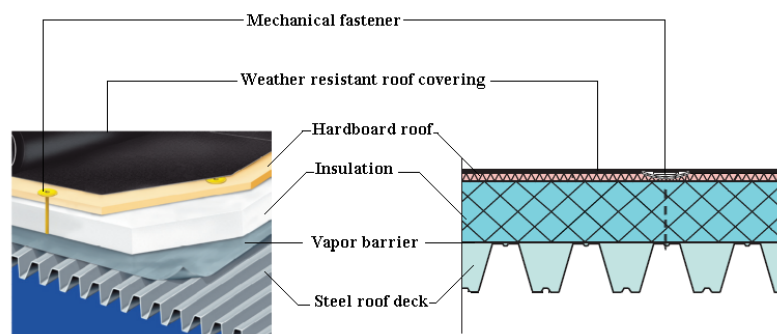


**Figure 1:** Basic components of insulated metal deck roofing (warm roof).

The steel deck is manufactured by cold forming from thinner steel sheet for providing the support to the insulations and enhancing the sound insulation. The steel sheeting is assembled with the wider flange on the top in order to provide more supporting area for the above insulations; and is attached to the underlying purlins or more commonly straight to the steel trusses by self-drilling or self-tapping screws. The insulation can be

one layer or multiple layers and covered with weather resistant roof covering. The insulations and covering roof are fixed to the steel roof deck with mechanical fasteners or with adhesives. In this paper, the insulations and covering roof are not included in the FE modeling.

### Profiles of steel sheeting

The profile of steel sheeting and its dimensions are shown in Figure 2. The thickness of the profile is 0.8 mm. When assembled as load-bearing decking, it is necessary to overlap edges of two sheets by putting the male edge of upper sheet inside female edge of lower sheet to make a side lap joint or to overlap ends of two sheet by laying one sheet over another sheet to make an end lap joint. When simulating a two span sheeting, an end lap joint at internal support is modeled with overlapping length of 600 mm. The span length is 6 m.

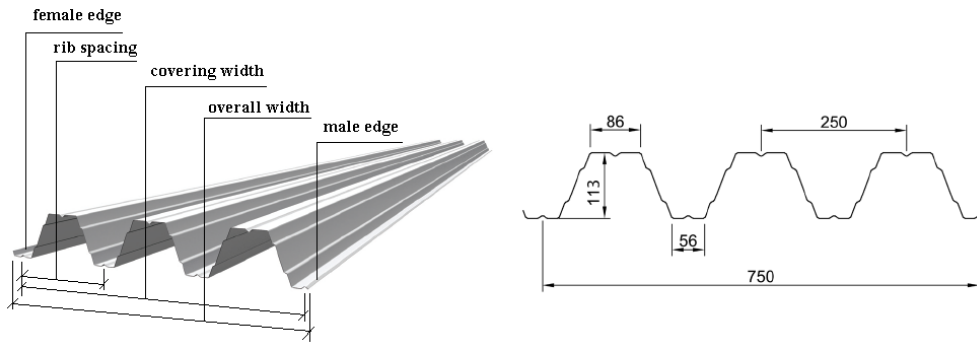


Figure 2: Steel sheeting and its dimensions.

### Loading

The loads applied to the sheeting include mechanical loading and thermal loading. According to Eurocode 0 (2002), fire is defined as accidental load and the combination factor for permanent load (with characteristic value of  $0.4 \text{ kN/m}^2$ ) is 1.0 and for main variable load, snow load (with characteristic value of  $1.8 \text{ kN/m}^2$ ) in this analysis, is 0.5. The ISO 834 fire curve is used as air temperature. Since the thickness of the sheeting is thin, the temperature of steel sheeting is assumed to be the same as air temperature. The distribution of mechanical loading is shown in Figure 3.

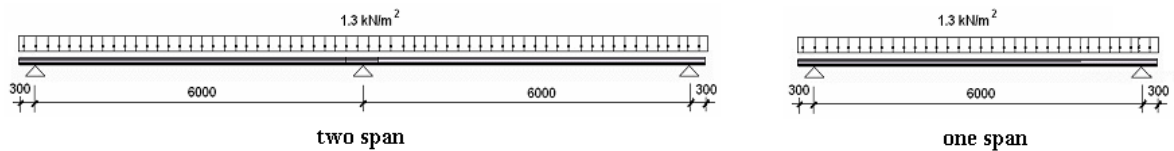
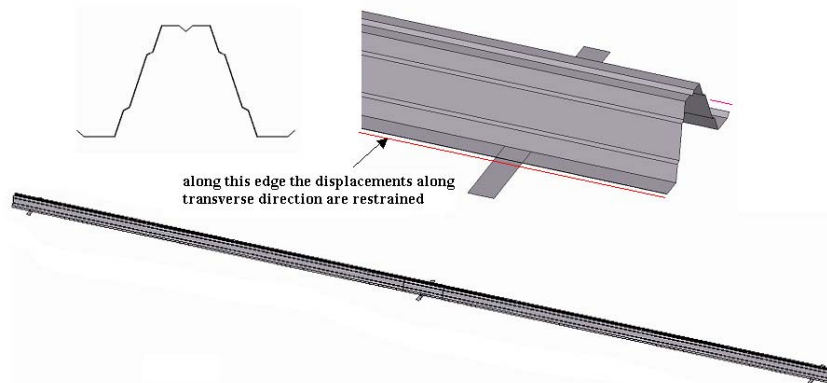


Figure 3: Mechanical loading.

## FINITE ELEMENT MODEL DESCRIPTIONS

Commercial FE software, ABAQUS Explicit, is used as an analysis tool. Only one rib is modeled for the sake of computing efficiency as shown in Figure 4. For two-span sheeting, the profile is connected to three rigid plates, which simulate the purlins or trusses underneath the roof system. The fasteners are assumed to be rigid when connecting sheeting to sheeting in side-lap joints and end-lap joints; and to three rigid plates. It is assumed that the material properties of rigid plates and fasteners are not affected by temperature.



**Figure 4:** FE modelling of one rib overlapping sheeting over two spans.

Thin shell elements with reduced integration S4R are used to model the steel sheeting. The quasi-static analysis procedure was adopted with a small enough dissipated energy fraction so that the energy fraction has no effects on the deflection behavior of sheeting. The two-step analysis is carried out, in which the mechanical loading was applied first (step 1) and then the temperatures were increased (step 2) as shown in Figure 5.

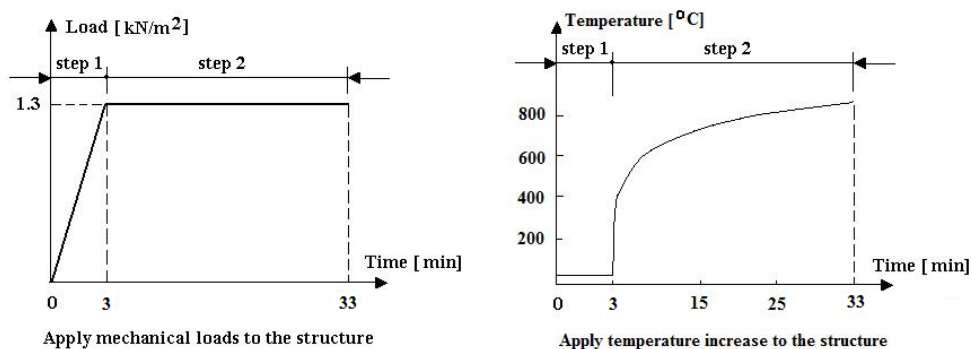


**Figure 5:** Mechanical loads and temperature increase to the structure.

The material of steel sheeting is S350GD+Z275 with the nominal yield strength  $350 \text{ N/mm}^2$ . The temperature dependent stress-strain curves and thermal elongation according to Eurocode 3, Part 1.2 (2005) are shown in Figure 6. In FE modelling, the decreasing phase of the material properties is not considered. According to the input requirements, the nominal stress-strain curves are transformed to the true stress-true strain curves. Similarly, total elongation coefficient is used via dividing the thermal elongation by its corresponding temperature.

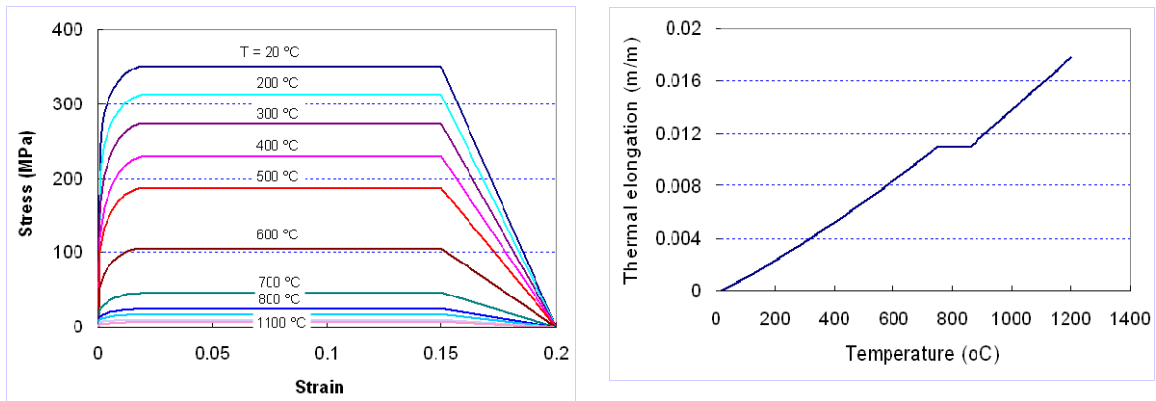


Figure 6: Material properties at elevated temperature and thermal elongation.

### VALIDATION OF FINITE ELEMENT MODEL

Sokol and Wald (2006) have investigated the behaviour of roof sheeting at elevated temperature via full scale testing. The testing is performed on sheeting with cantilever end simulating the case continuously over two spans. The sheeting is heated under the simply supported part as shown to the left in Figure 7, which also shows the dimension of the profile and connecting details to the support. The measured material properties are  $f_y = 372 \text{ N/mm}^2$  and  $f_u = 412 \text{ N/mm}^2$ . The displacement history at mid-span (no information about position of measuring point of the cross-section) under mechanical loading ( $0.85 \text{ kN/m}^2$ ) is shown in Figure 7 in the middle.

Figures 7 to the right show the displacement histories at mid-span of left span from FE analysis, respectively. In FE modelling, the sheeting is overlapping at mid-support with span 1 on the top of span 2 and is heated underneath both spans. The sheeting deforms first under mechanical load (up to 3 minutes). The displacement histories show very good agreement with that from above mentioned testing. The deformation is a little upward in the beginning. Then the sheeting deforms downward dramatically. Thereafter, the displacements increase with slower rates. When comparing to deflection on the top flange from FE analysis, it is about the same scale as that from the tests.

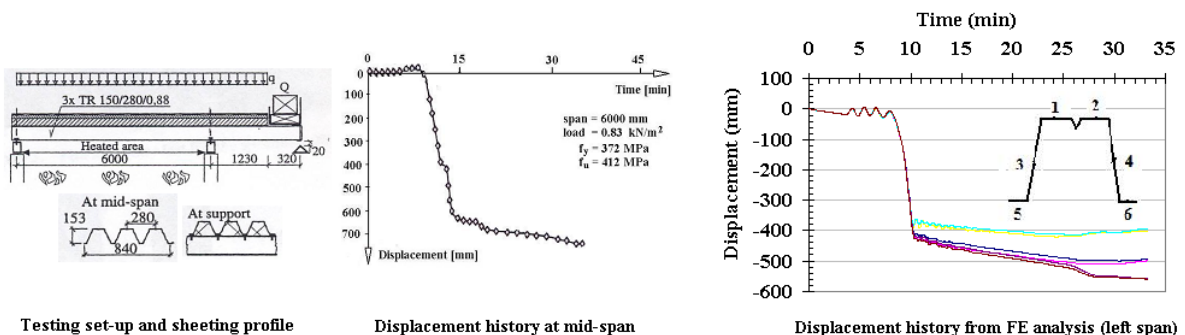


Figure 7: Testing and displacement history by Sokol and Wald (2006).

## RESULTS OF FINITE ELEMENT ANALYSIS

### ***Deformation histories***

Due to the thermal elongation and the restraints when connecting the lower flange to the support, the axial compression forces are generated and the lower parts of the profile are in compression. The upper flange without any restraints at both end supports expands freely. The local buckling occurred upwards near two end supports. A hinge developed at the buckling point and the steel sheeting cannot carry higher axial load. No local buckling occurred in the mid-support because of relatively high stiffness when overlapping of sheeting profiles (Figure 8,  $t = 3$  minutes).

The material properties degrade with increased temperature, the sheeting starts to deform downward under the transversally applied mechanical loads, which cause hogging bending moment in the internal support. Local buckling occurred at intersection of single profile and overlapping profiles in the span 1 near the internal support. Another hinge is created and hogging moment is released. Both spans behave like two simply supported beams (Figure 8,  $t = 6$  minutes).

With the further degradation of material properties, the sheeting deforms further. When the distance shortening between two supports overtake the lateral deflection, tension forces develop at supports; the sheeting profile starts to open at mid-span (Figure 8,  $t = 15$  minutes, one moment during the opening). When the temperature rises further, the sheeting deforms more. The profiles are totally open over the whole span (Figure 8,  $t = 30$  minutes).

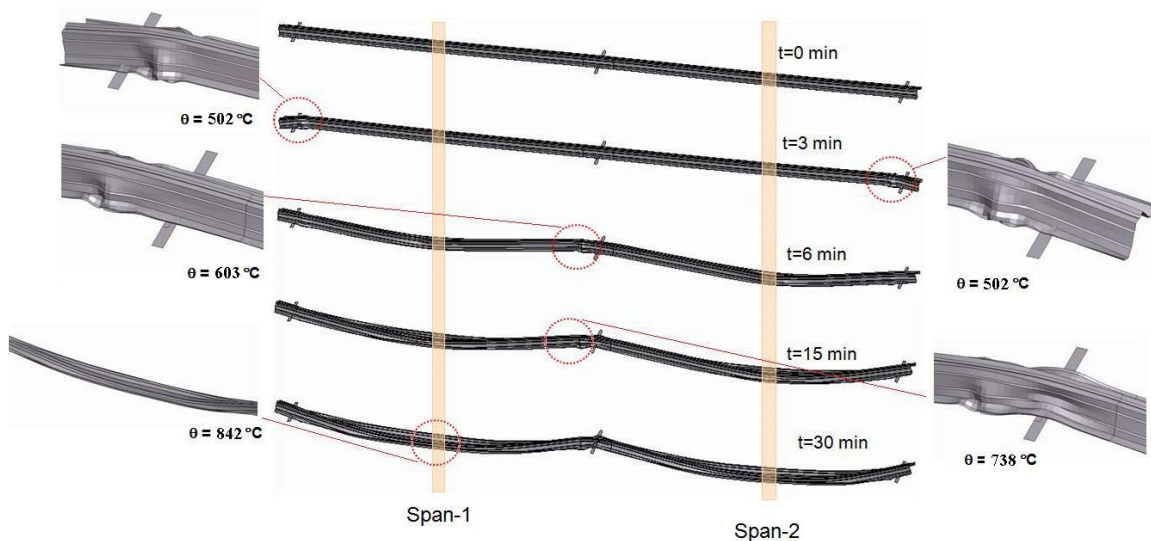


**Figure 8:** Deformation histories and local buckling modes.

### ***Displacements in the mid-spans***

The displacements oscillate around the initial displacement because transversely applied load competes with secondary order effect of axial compression force on upward

deformation. When the local buckling near mid-support occurred, another hinge developed near the internal support. The sheeting deformed rapidly downwards in the mid-span until the tension forces develop at supports. Since the upward buckling near internal support in span-1 and continuity of the whole sheeting over two spans, the sheeting in span-2 deformed more than that of in span-1 (Figure 9). When the sheeting is in catenary action, the profile opens; top flange, web and bottom flange deform separately. Thereafter, the deflections increased further with a steady gradient until the sheeting profile along each span opens totally.

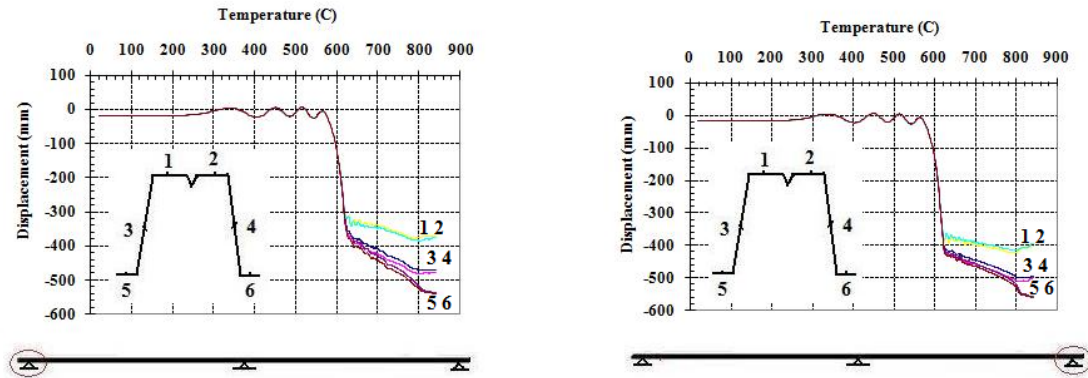


Figure 9: Displacement history by FE analysis.

### Axial force history in supports

Figure 10 shows the axial forces developed at left and right end supports. The value in each figure is the sum of two fasteners at each support. Due to the thermal expansion and restraints from fasteners connected to the supports, the axial compression force developed first. Because of the fasteners are assumed to be rigid, the values of the compression forces increase rapidly with temperature rising until the local buckling occurred at end supports.

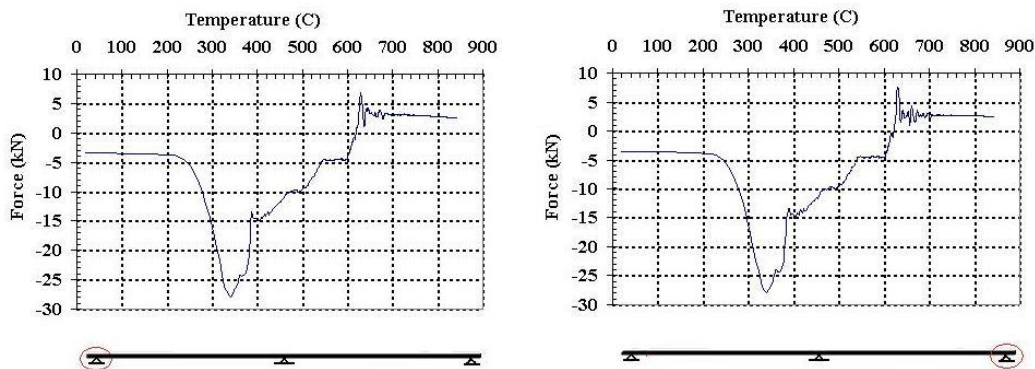


Figure 10: Axial force developed at two end supports by FE analysis.

The compressive axial force is released due to large displacement promoted by post-buckling and the plastic straining (with decreasing material strength). The upward deformation created by thermal expansion and fixing of bottom flange to the supports

cancels out the downward deflection produced by transversally applied load. Therefore, the compression force reduces dramatically similar to a straight column buckling. When the sheeting deforms further downwards due to the overtaking of mechanical loading, the hinge developed near the internal support releases the hogging moment in the internal support. Thereafter, the tensile axial force developed because the lateral deflection become sufficiently large, the shortening of sheeting length overtook the thermal expansion. The sheeting is now in catenary action, i.e. a small component of the tension carries the transverse load directly.

### Comparisons with single-span sheeting

When comparing the mid-span displacement of one-span sheeting to that of two-span sheeting, three differences are observed (Figure 11): the maximum upward displacement is larger in one-span sheeting; the starting time for downward displacement is delayed for two-span sheeting; the displacement, when the profile is opening, is less for one-span sheeting. The main reason for these differences is that continuity in the internal support provides the restraints for the displacement.

Similarly, the restraints from the internal support delay the transforming of compression force to tension force and increase the value of tension force in two-span sheeting. The maximum compression forces developed at the supports for both cases are the same because the initial buckling occurred near the end support.

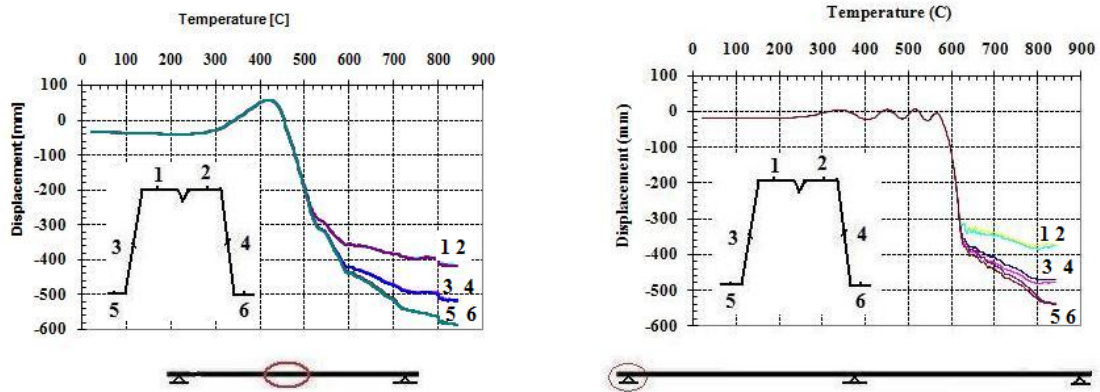
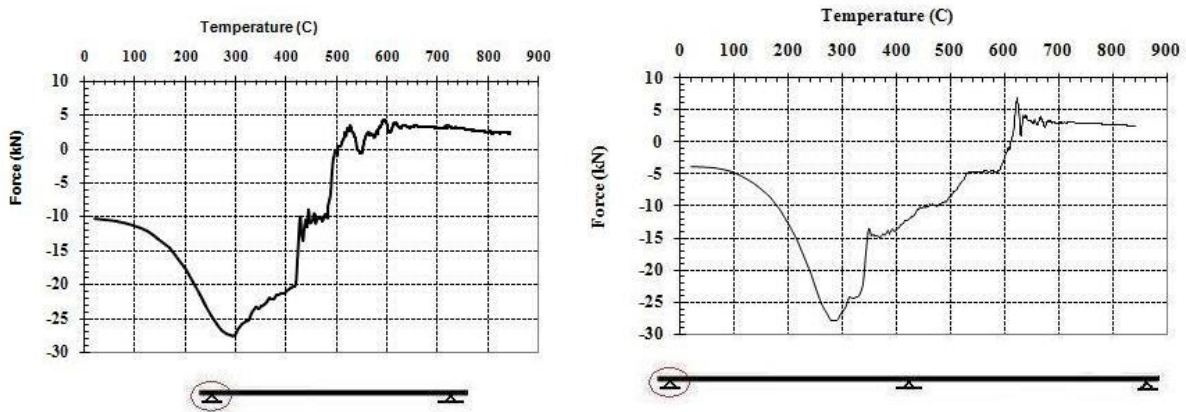


Figure 11: Comparisons of mid-span displacement of one span to two span sheeting.



## CONCLUSIONS AND FUTURE RESEARCHES

3-D finite element model incorporating geometric non-linearity and non-linear material properties have been used to analyse the behaviour of two-span sheeting with overlaps in the mid-support in fire. In the beginning, the sheeting structure bent and buckled upwards first due to thermal expansion and axial restraints when connecting the sheeting to the supports, which causes high compression force in the structure. After that the structure deforms rapidly downwards with high deformation due to stiffness degradation with increasing temperature. The catenary force in the structure has significant role to sustain the applied load. Small tensile force can sustain the transversally applied load. No run-away deformation happened before 30 minutes in this analysis. It can be concluded that the sheet itself can stand for 30 minutes fire, assumed that the steel temperature is the same as air. When comparing the displacement and axial forces at supports with one-span sheeting, the restraints coming from the continuity in the internal support in two-span sheeting delay the transformation to tensile force, lessen the maximum displacement developed in the mid-span and increase the maximum value of tensile force.

It has been shown in the analysis that the connection is first under compression force due to thermal expansion and then under tension in catenary action. The rigid connections were used and no failures in the connections were assumed. The behaviour of connection in fire should be included in future researches. Besides, the real fire model should be refined instead of using ISO fire curve.

## ACKNOWLEDGEMENTS

This research was financially supported by Rautaruukki Oyj.

## REFERENCES

- ABAQUS on-line documentations, version 6.6.
- Allam, A.M., Burgess, I.W., Plank R.J. (2002). Performance-based simplified model for a steel beam at large deflection in fire. Proceeding of 4<sup>th</sup> international conference on performance-based codes and fire safety design methods, Melbourne, Australia.
- E.C.S.S., TWG 7.3 (1983), European recommendations for steel construction: good practice in steel cladding and roofing, CONSTRDO.
- EN 1990 (2002), Eurocode 0: Basis of structural design.
- EN 1993-1-2 (2005), Eurocode 3: Design of steel structures, Part 1.2: General rules – structural fire design.
- Liu, T.C.H., Fahad, M.K., Davies, J.M. (2001). Catenary effect in axially restrained steel beam in fire. Proceeding of 1<sup>st</sup> International conference on steel and composite structures, Pusan, Korea, 2, 1669-1708.
- Liu, T.C.H., Fahad, M.K., Davies, J.M. (2002). Experimental investigation of behaviour of axially restrained steel beams in fire. Journal of Constructional Steel Research, 58(9), 1211-1230.

Rotter, J.M. and Usmani A.S. (2000). Fundamental principles of structural behaviour under thermal effects. Proceedings of 1<sup>st</sup> international workshop on structures in fire, Copenhagen, Demark, 1-20.

Sokol, Z., Wald, F., Pincemaile, S. (2006). Structural integrity of corrugated sheets exposed to fire. Steel- a new and traditional material for building, edited by Dubina and Ungureanu, Taylor & Francis Group, London, 561-566.

Usmani, A.S, Rotter, J.M., Lamont, S. Sanad, A.M., Gillie, M. (2001). Fundamental principles of structural behaviour under thermal effects. Fire Safety Journal, 36(8), 721-744.

Wang, Y.C. (2002). Steel and composite structures: behaviour and design for fire safety, Spon Press, Taylor & Francis Group, London and New York.

Wang, Y.C., Yin, Y.Z. (2006). A simplified analysis of catenary action in steel beam in fire and implications on fire resistant design. Steel and Composite Structures, 6(5), 367-386.

Wong, M.B. (2005). Modelling of axial restraints for limiting temperature calculation of steel members in fire. Journal of Constructional Steel Research, 61(5), 675-687.

Yin, Y.Z., Wang, Y.C. (2004). A numerical study of large deflection behaviour of restrained steel beams at elevated temperatures. Journal of Constructional Steel Research, 60(7), 1029-1047.

Zalosh, R.G. (2003). Industrial fire protection engineering, WILEY, UK.

Wei Lu, University Teacher,  
D.Sc. (Tech.)

Pentti Mäkeläinen, Professor,  
D.Sc. (Tech.)

Jyri Outinen, R&D Manager  
D.Sc. (Tech.)

Laboratory of Steel Structures, TKK  
PL 2100, Fi-02015, TKK, Finland  
Email: Wei.Lu@tkk.fi

Laboratory of Steel Structures, TKK  
PL 2100, FI-02015, TKK, Finland  
Email: Pentti.Makelainen@tkk.fi  
Ruukki Construction, Rautaruukki Oyj  
P.O.Box 35, FI-01531 Vantaa, Finland  
Jyri.Outinen@ruukki.com